Received: 13 July 2021 | Revised: 21 December 2021 | Accepted: 22 December 2021

DOI: 10.1111/cas.15261

Cancer Science WILEY

ORIGINAL ARTICLE

Complement C1q binding protein regulates T cells' mitochondrial fitness to affect their survival, proliferation, and anti–tumor immune function

Hui Tian[1] | Gang Wang[1] | Qiping Wang[2] | Baofu Zhang[1] | Guan Jiang[3] | Huizhong Li[1] | Dafei Chai[1] | Lin Fang[1] | Meng Wang[1] | Junnian Zheng[1,4,5]

[1]Cancer Institute, Xuzhou Medical University, Xuzhou, China

[2]Jiangyin Clinical Medical College, Jiangsu University, Jiangyin City, China

[3]Department of Dermatology, Affiliated Hospital of Xuzhou Medical University, Xuzhou, China

[4]Center of Clinical Oncology, Affiliated Hospital of Xuzhou Medical University, Xuzhou, China

[5]Jiangsu Center for the Collaboration and Innovation of Cancer Biotherapy, Cancer Institute, Xuzhou Medical University, Xuzhou, China

Correspondence
Junnian Zheng and Hui Tian, Cancer Institute, Xuzhou Medical University, Xuzhou, Jiangsu 221002, China.
Emails: jnzheng@xzhmu.edu.cn (JZ); huitian@xzhmu.edu.cn (HT)

Funding information
National Natural Science Foundation of China, Grant/Award Number: 82073012, 81871869 and 81872488; Key University Science Research Project of Jiangsu Province, Grant/Award Number: 19KJA470001 and 19KJA580001

Abstract

T cells survival, proliferation, and anti–tumor response are closely linked to their mitochondrial health. Complement C1q binding protein (C1QBP) promotes mitochondrial fitness through regulation of mitochondrial metabolism and morphology. However, whether C1QBP regulates T cell survival, proliferation, and anti–tumor immune function remains unclear. Our data demonstrated that C1QBP knockdown induced the accumulation of reactive oxygen species (ROS) and the loss of mitochondrial membrane potential to impair T cell mitochondrial fitness. At the same time, C1QBP insufficiency reduced the recruitment of the anti–apoptotic proteins, including Bcl-2 and Bcl-XL, and repressed caspase-3 activation and poly (ADP-ribose) polymerase cleavage, which consequently accelerated the T cell apoptotic process. In contrast, C1QBP knockdown rendered T cells with relatively weaker proliferation due to the inhibition of AKT/mTOR signaling pathway. To investigate the exact role of C1QBP in anti–tumor response, $C1QBP^{+/-}$ and $C1QBP^{+/+}$ mice were given a subcutaneous injection of murine MC38 cells. We found that C1QBP deficiency attenuated T cell tumor infiltration and aggravated tumor-infiltrating T lymphocytes (TIL) exhaustion. Moreover, we further clarified the potential function of C1QBP in chimeric antigen receptor (CAR) T cell immunotherapy. Our data showed that $C1QBP^{+/-}$ CAR T cells exhibited relatively weaker anti–tumor response than the corresponding $C1QBP^{+/+}$ CAR T cells. Given that C1QBP knockdown impairs T cells' anti–apoptotic capacity, proliferation as well as anti–tumor immune function, development of the strategy for potentiation of T cells' mitochondrial fitness through C1QBP could potentially optimize the efficacy of the related immunotherapy.

KEYWORDS
anti–tumor immune function, C1QBP, mitochondrial fitness, proliferation, T cells survival

Hui Tian and Gang Wang contributed equally to this work.

1 | INTRODUCTION

The immune system has evolved multiple cellular mechanisms for the detection and elimination of transformed cells. During the course of an immune response, naive T cells recognize tumor antigen, rapidly proliferate, and subsequently produce a variety of effector molecules, which leads to tumor regression.[1-3] At the same time, tumor cells generate an immunosuppressive microenvironment to restrict T cell proliferation, survival, and effector function through direct repression as well as the recruitment of immunosuppressive populations tasked with maintaining immune tolerance.[4-6] Therefore, a successful immune response relies on T cells with extensive proliferation, robust effector function as well as long-term lifespan.

Mitochondria are essential hubs of metabolic activity to meet the increased bioenergetic and biosynthetic demands following T cell activation and proliferation.[6-8] Once T cells are activated by antigenic substances, they rapidly expand and proliferate through synthesizing high levels of cytokines and delivering cytotoxic payload to target cells. Recent studies show that T cell proliferation and longevity are closely linked to mitochondrial fitness, suggesting that mitochondria represent the key organelles by which the fate and function of T cells can be regulated and determined.[7,9,10] Complement C1q binding protein (C1QBP), as an evolutionarily conserved and multifunctional protein, is predominately localized to the mitochondrial matrix. It has been reported that C1QBP, as an important mitochondrial regulator, is involved in mitochondrial metabolism and function.[11-14] Mouse embryonic fibroblasts (MEF) isolated from C1QBP knockout embryos are characterized by severely impaired ATP production and reduced mitochondrial membrane potential.[15] Moreover, C1QBP silencing changed mitochondrial morphology from fusion with the linear and tubular networks to fission with the discrete and fragmented phenotypes.[16,17] Therefore, C1QBP is regarded to be implicated in the maintenance of mitochondrial integrity and dynamics, which determines mitochondrial fitness.[8-10] Recently, C1q, as the identified ligand of C1QBP, was reported to be associated with $CD8^+$ T cell differentiation and survival.[18] However, whether C1QBP, as an important sustainer of mitochondrial fitness, plays an indispensable role in T cell longevity and proliferation as well as anti–tumor immune function remains unclear.

Given that C1QBP-knockout mice exhibited midgestation lethality due to the dysfunction of the mitochondrial respiratory chain and the fatal deficiency of mitochondrial protein translation,[15] here we isolated T cells from mice with one allele of C1QBP knockout and found that $C1QBP^{+/-}$ T cells had diminished proliferation in response to the T cell receptor (TCR)-mediated antigen activation. At the same time, C1QBP knockdown caused T cells to lose mitochondrial membrane potential and be susceptible to apoptosis in the context of the reactive oxygen species (ROS)-induced stress. To further investigate the underlying molecular mechanism, we assessed the Bcl-2 anti–apoptotic signaling pathway and found that C1QBP knockdown induced T cells with less accumulation of the anti–apoptotic proteins, such as Bcl-2 and Bcl-XL, thus triggering caspase-3 activation and poly (ADP-ribose) polymerase (PARP) cleavage to initiate T cells apoptosis.

To delineate the specific role of C1QBP in T cells' anti–tumor immune function, murine colon adenocarcinoma MC38 cells were injected into $C1QBP^{+/+}$ and $C1QBP^{+/-}$ mice. Our data showed that $C1QBP^{+/-}$ mice had relatively weaker tumor repression when compared to $C1QBP^{+/+}$ mice. $C1QBP^{+/-}$ T cells also exhibited less tumor infiltration and more exhausted phenotype than $C1QBP^{+/+}$ T cells. To confirm the exact function of C1QBP in T cell-related immunotherapy, we constructed the chimeric antigen receptor (CAR)-T cells targeting human B7-H3 (huB7-H3) antigen with different amounts of C1QBP to test whether C1QBP would impact the immunotherapeutic efficacy of CAR T cells. Our data demonstrated that C1QBP knockdown dampened the anti–tumor immune function of CAR T cells in vivo and in vitro.

Because the enhancement of T cells' mitochondrial health and function has been gradually regarded to the improvement of current and developing immunotherapies, understanding how C1QBP regulates T cell proliferation, survival, and anti–tumor immune function through maintaining mitochondrial fitness is of broad interest and clinical importance.

2 | MATERIALS AND METHODS

2.1 | Mice

Complement C1q binding protein heterozygous mice were donated by Dr Yanping Zhang from the Department of Radiation Oncology and Lineberger Comprehensive Cancer Center, the University of North Carolina, USA. C1QBP heterozygous ($C1QBP^{+/-}$) and wild-type ($C1QBP^{+/+}$) mice were on a C57BL/6 background.[19] All mice were housed and bred in the specific pathogen-free animal facility of the Experimental Animal Center, Xuzhou Medical University, China.

2.2 | Antibodies and reagents

Rabbit anti–C1QBP (cat. #24474-1-AP), anti–Caspase3 (cat. #19677-1-AP), anti–Bcl-XL (cat. #10783-1-Ap), anti–Bax (cat. #50599-2-Ig), anti–Puma (cat. #55120-1-AP), anti–Bcl-2 (cat. #12789-1-AP), anti–PARP (cat. #13371-1-AP), anti–Ki67 (cat. #27309-1-AP), anti–AKT (cat. #10176-2-AP), anti–mTOR (cat. #20657-1-AP), anti–Raptor (cat. #20984-1-AP), anti–p70(S6K) (cat. #14485-1-AP), anti–CD3 (cat. #17617-1-AP), and mouse anti–β-Actin (cat. #60008-1-Ig) were purchased from Proteintech. Rabbit anti–phospho-Akt (Ser473) (cat. #4060), anti–phospho-mTOR (Ser2448) (cat. #5536), anti–phospho-Raptor (Ser792) (cat. #2083), anti–phospho-p70S6 Kinase (Ser371) (cat. #9208), anti–CD8α (cat. #98941) and anti–CD4 (cat. #25229) antibodies were purchased from Cell Signaling Technology. Moreover, PerCP-anti–mouse-CD4 (cat. #100538), APC-anti–mouse-CD8α (cat. #100712), FITC-anti–mouse-CD3ε (cat. #100306), PE-Cy7-anti–mouse-CD3ε (cat. #100320), PE-Cy7-anti–mouse-CD45 (cat.

#147704), PE-anti–mouse-PD-1 (cat. #109103), PE-anti–mouse-LAG-3 (cat. #125207), and PE-anti–mouse-Tim-3 (cat. #119703) antibodies were purchased from BioLegend.

2.3 | T cell isolation and culture

The spleens of 6-to 8-week-old C1QBP$^{+/-}$ and C1QBP$^{+/+}$ C57/BL6 mice were harvested, gently ground in MACS buffer (PBS + 0.5% BSA + 2 mM EDTA) and then passed through a sterile 40-μm nylon filter (BD Falcon). Red blood cells were lysed with RBC Lysing Buffer (BioLegend). The murine T cells were isolated by Pan T magnetic Microbeads (Miltenyi Biotec) from splenocytes obtained from C1QBP$^{+/+}$ and C1QBP$^{+/-}$ mice. CD4$^+$ or CD8$^+$ T cells were sorted on a FACSAria III Cell Sorter (BD Biosciences) and planted in 24-well plates coated with 2.5 μg/mL anti–CD3ε (145-2C11, Bio-X-Cell) and 1 μg/mL anti–CD28 antibodies (37.51 Bio-X-Cell). All the above cells were cultured in RPMI-1640 medium (Corning) supplemented with 10% FBS, 4 mM L-glutamine, 1% penicillin/streptomycin, 2 ng/mL IL-2, 10 ng/mL IL-7, 5 ng/mL IL-15, and 75 μM β-mercaptoethanol and incubated at 37°C in a 5% CO_2 humidified atmosphere.

2.4 | Immunoblot analysis

Immunoblot analysis was performed as described previously.[20] The lysates of T cells were prepared in 0.5% NP-40 lysis buffer (50 mM Tris-HCl, pH 7.4, 150 mM NaCl, 2 mM EDTA, 2 mM EGTA, 0.2% Triton X-100, 0.5% NP-40, and protease inhibitor cocktail) and separated on 12% SDS/PAGE gel. The proteins were transferred to nitrocellulose membranes and then immunoblotted using the primary antibodies overnight at 4°C. Membranes were washed with PBST, incubated with the appropriate HRP-conjugated anti–mouse or anti–rabbit secondary antibodies in 5% (w/v) non–fat dried skimmed milk powder/PBST, and visualized using enhanced chemiluminescence reagents (Thermo Scientific) according to the manufacturer's instructions.

2.5 | Immunohistochemistry

The tumors were fixed in 10% neutral buffered formalin and included in paraffin, which was performed as described previously.[21] The slides were incubated in 3% hydrogen peroxide for 20 minutes to quench endogenous peroxidases. Next, the sections were washed and incubated in the relevant primary antibodies including anti–Ki67 (1:4000 dilution), anti–Puma (1:200 dilution), anti–CD4 (1:100 dilution), and anti–CD8α (1:400 dilution) antibodies overnight at 4°C. The slides were then incubated with the enhancer solution for 20 minutes at room temperature, followed by the secondary antibody (Beijing Zhongshan Jinqiao Biotechnology) for 30 minutes. Diaminobenzidine tetrahydrochloride (DAB) solution (Beijing Zhongshan Jinqiao Biotechnology) was added for visualization. Immunoreactivity was observed using an Olympus BX51 microscope and captured using Camedia Master C-3040 digital camera.

2.6 | Flow cytometry and analyzation

For preparation of single cell suspensions, tumor tissues were mechanically dissected and washed with PBS. The cell suspension was passed through a sterile 40-μm nylon filter (BD Falcon). A single-cell suspension was obtained, and 0.5-1 × 10^6 cells were collected and stained with PerCP-anti–mouse-CD4 and APC-anti–mouse-CD8α antibodies to detect the percentage of CD4$^+$ and CD8$^+$ T cell tumor infiltration. Next, to further examine tumor infiltrating T cell exhaustion, the cell suspensions continued to be stained by PE-anti–mouse-PD-1, PE-anti–mouse-LAG-3, or PE-anti–mouse-Tim-3 antibodies, respectively. Finally, these stained cells were analyzed on the FACSCanto II Flow Cytometer (BD Biosciences), and FACS data were analyzed with FlowJo software (TreeStar).

2.7 | T cell proliferation assay

For carboxyfluorescein succinimidyl ester (CFSE) dilution assay, the isolated T cells were labeled in 2 μM CFSE (Life Technologies, C1157) for 10 minutes and then washed with 10 volumes of PBS. Stained T cells were seed on in 24-well plates coated with anti–CD3ε/CD28 antibodies and cultured in RPMI-1640 medium supplemented with 10% FBS, 4 mM L-glutamine, 1% penicillin/streptomycin, 75 μM β-mercaptoethanol, 2 ng/mL IL-2, 10 ng/mL IL-7, and 5 ng/mL IL-15, under 5% CO_2, atmospheric oxygen, at 37°C in a humidified incubator. After 1, 2, and 3 days, T cells were harvested and analyzed with a FACSCanto II Flow Cytometer.

2.8 | T cell apoptosis assays

The apoptotic rate of T cells was assayed using an Annexin V-FITC Apoptosis Detection Kit (NanJing KeyGen Biotech). The treated T cells were briefly washed with ice-cold PBS twice and resuspended in 200 μL binding buffer containing 5 μL Annexin V-FITC for 15 minutes and then in 300 μL binding buffer containing 5 μL propidium iodide (PI) for 5 minutes at room temperature in the dark. After incubation, these T cells were analyzed using a FACSCanto II Flow Cytometer.

2.9 | Mitochondrial membrane potential assay

For evaluation of mitochondrial membrane potential of T cells, the treated T cells were incubated in 500 μL of 1 μM JC-10 working solution (NanJing KeyGen Biotech) at 37°C in a 5% CO_2 incubator for 30 minutes, protected from the light. Both FL1-FITC channel (green fluorescent monomeric signal) and FL2-PE channel (orange fluorescent aggregated signal) can be detected using a FACSCanto II Flow Cytometer. A tetramethylrhodamine methyl ester (TMRM) assay was also used to assess the mitochondrial membrane potential. The treated T cells were stained with TMRM (T668; ThermoFisher) for 30 minutes at 37°C and then analyzed using a FACSCanto II Flow Cytometer.

2.10 | Reactive oxygen species assay

To detect the ROS levels of C1QBP$^{+/+}$ and C1QBP$^{+/-}$ T cells in response to the TCR activation or the oxidative stress, the treated T cells were stained with 2′,7′-dichlorofluorescin diacetate (DCFDA, also known as H2DCFDA, D399; ThermoFisher) for 10 minutes at 37°C. After incubation, these cells were analyzed using a FACSCanto II Flow Cytometer.

2.11 | MC38-induced xenograft mouse models

The murine colon carcinoma MC38 cells were transduced with lentiviral particles carrying firefly luciferase (Luc) and the puromycin resistance gene. After 48 hours, the positive MC38 cells expressing firefly luciferase were screened with 1 μg/mL puromycin. The selected positive Luc-MC38 cells (2×10^5) were injected subcutaneously into the flanks of 2-month old C1QBP$^{+/+}$ and C1QBP$^{+/-}$ mice (five mice per group). Tumor volume (width × length × width/2; cm^3) was determined with calipers. After 21 days, these mice were humanely euthanized by CO_2 asphyxiation. The corresponding tumor tissues were collected for flow cytometry analysis or were fixed in formalin for immunohistochemistry. All animal experiments were approved by the Animal Care Committee of the Xuzhou Medical University.

2.12 | Generation of C1QBP$^{+/+}$ and C1QBP$^{+/-}$ chimeric antigen receptor T cells targeting huB7-H3

To prepare the targeted huB7-H3 CAR T cells, we first constructed the retroviruses expressing huB7-H3 CAR. Briefly, the chimeric antigen receptor was pieced together using portions of the humanized B7-H3 (8H9 clone 3.1) single chain variable fragment and the published portions of the murine CD28 and CD3ζ sequences.[22] The huB7-H3 CAR cassettes were ligated into the mouse stem cell virus-based splice-gag vector (MSCV) retroviral vector. Next, the 293T cells were co–transfected with huB7-H3 CAR MSCV vector and pCL-Eco helper vector. The supernatant containing the CAR retrovirus targeting huB7-H3 antigen were collected 48 hours later and filtered with a 0.22-μm filter. Next, we generated the murine CAR T cells targeting huB7-H3. The murine T cells obtained from splenocytes of C1QBP$^{+/+}$ and C1QBP$^{+/-}$ mice were stimulated by the anti–CD3ε/CD28 antibodies for 24 hours. The activated T cells were then transduced with the above retroviral supernatants using retronectin-coated plates (Takara Bio). The transfection of murine T cells was performed according to the previous protocols.[23] After removal from the retronectin-coated plates, T cells were expanded in RPMI-1640 medium. After 48 hours, the murine CAR T cells targeting huB7-H3 were collected and used for the next functional assays.

2.13 | Murine MC38 cell line expressing huB7-H3 antigen

To establish murine MC38 cells stably expressing huB7-H3 antigen, MC38 cells were transduced with the lentiviral particles carrying the open reading frame of 4Ig-B7-H3 (GenBank: NM_001024736), Luc, and green fluorescent protein (GFP). After 48 hours, the positive huB7-H3 MC38 cells expressing Luc and GFP were screened with 1 μg/mL puromycin and used for the next experiment.

2.14 | Co–culture experiments

The huB7-H3 MC38 cells marked by GFP were seeded in 24-well plates at a concentration of 2×10^5 cells/well for 24 hours. C1QBP$^{+/+}$ and C1QBP$^{+/-}$ CAR T cells targeting huB7-H3 antigen were added to the culture at different effector to target ratios (E:T = 1:2 or 1:1) without the addition of exogenous cytokines. At the same time, their corresponding control groups were set up through the non–transduced C1QBP$^{+/+}$ or C1QBP$^{+/-}$ T cells co–cultured with huB7-H3 MC38 cells (E:T = 1:2). After 6 hours of co–culture, the residual amount of huB7-H3 MC38 cells (marked by GFP) and the control T cells or CAR T cells (identified by PE-Cy7-CD3) were analyzed by FACS. Dead cells were gated out by Zombie Aqua Dye (Biolegend) staining.

2.15 | ELISA

The CAR T cells targeting huB7-H3 were co–cultured with huB7-H3 MC38 tumor cells (2×10^5 cells/well) in 24-well plates at different effector to target ratios (E:T = 1:2 or 1:1) without the addition of exogenous cytokines. After 6 hours, the supernatant was collected, and cytokines (IFN-γ and TNF-α) were measured in duplicate using specific ELISA kits (Proteintech) following the manufacturer's instructions.

FIGURE 1 Complement C1q binding protein (C1QBP) knockdown induces the increase of reactive oxygen species (ROS) and the decrease of mitochondrial membrane potential ($\Delta\Psi_M$). T cells isolated from C1QBP$^{+/+}$ and C1QBP$^{+/-}$ mice were stimulated with anti–CD3/CD28 antibodies for 24 or 48 h or stimulated with anti–CD3/CD28 antibodies for 24 h and then treated with the different doses of H_2O_2 for 30 min. A, ROS levels of C1QBP$^{+/+}$ and C1QBP$^{+/-}$ T cells in response to TCR activation or H_2O_2-induced oxidative stress were detected through by 2′,7′-dichlorofluorescin diacetate (DCFDA) assa ys. B, $\Delta\Psi_M$ of C1QBP$^{+/+}$ and C1QBP$^{+/-}$ T cells in response to T cell receptor (TCR) activation or H_2O_2 treatment were evaluated by tetramethylrhodamine methyl ester (TMRM) assay. C, $\Delta\Psi_M$ of CD4$^+$ and CD8$^+$ T cells from C1QBP$^{+/+}$ and C1QBP$^{+/-}$ mice under TCR activation or H_2O_2 treatment were measured through JC-10 assay. Data are means ± standard deviation (SD) from three independent experiments (n = 3); $^{**}P < .01$, $^{*}P < .05$

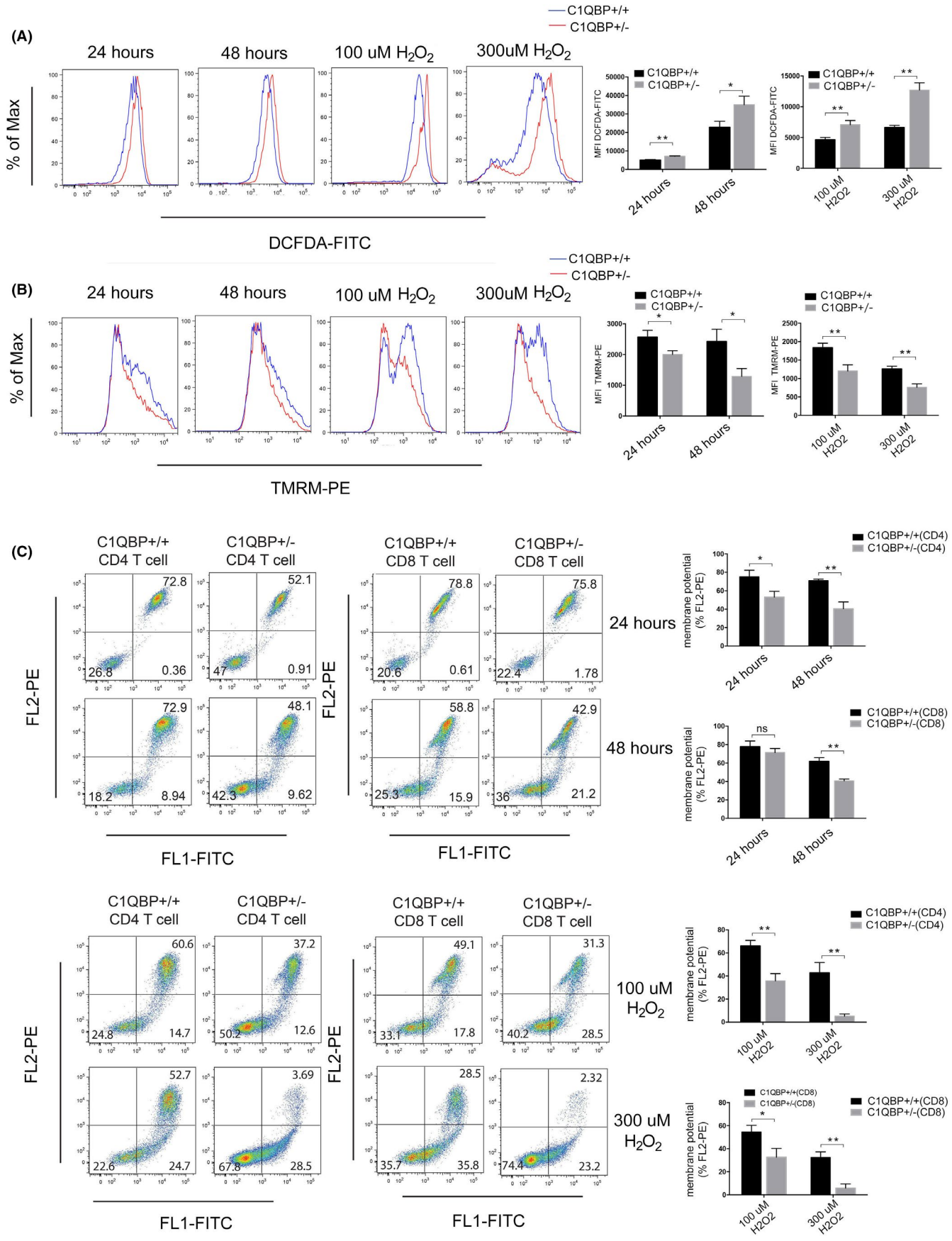
(A)
C1QBP+/+
C1QBP+/-
24 hours
48 hours
100 uM H2O2
300uM H2O2
% of Max
DCFDA-FITC
MFI DCFDA-FITC
(B)
TMRM-PE
MFI TMRM-PE
(C)
C1QBP+/+ CD4 T cell
C1QBP+/- CD4 T cell
C1QBP+/+ CD8 T cell
C1QBP+/- CD8 T cell
FL2-PE
FL1-FITC
72.8
26.8
0.36
52.1
47
0.91
78.8
20.6
0.61
75.8
22.4
1.78
72.9
18.2
8.94
48.1
42.3
9.62
58.8
25.3
15.9
42.9
36
21.2
60.6
24.8
14.7
37.2
50.2
12.6
49.1
33.1
17.8
31.3
40.2
28.5
52.7
22.6
24.7
3.69
67.8
28.5
28.5
35.7
35.8
2.32
74.4
23.2
membrane potential (% FL2-PE)
C1QBP+/+(CD4)
C1QBP+/-(CD4)
C1QBP+/+(CD8)
C1QBP+/-(CD8)
ns

2.16 | Tumor model and chimeric antigen receptor T cell treatment

In an adoptive CAR T cell transfer animal model, the huB7-H3 MC38 cells expressing Luc (1×10^6) were subcutaneously (sc) engrafted into one flank of C57BL/6 mice on Day 0. On Day 9, 200 mg/kg cyclophosphamide was injected intraperitoneally 1 day before acceptance of adoptive transfer of CAR T cells. One day later, the murine C1QBP$^{+/+}$ and C1QBP$^{+/-}$ CAR T cells targeting huB7-H3 (4×10^6) were adoptively transferred intravenously (iv) into acceptor C57BL/6 mice bearing the huB7-H3 MC38 tumor cells. The progress of tumor growth was monitored by measuring the bioluminescence signal or calculating tumor volumes using the vernier caliper.

2.17 | Animal experiments guidelines

All animal experiments were carried out in compliance with the guidelines of Xuzhou Medical University Animal Care and Use Committee following an approved Animal Utilization Project Protocol (AUPP #SYXK0030) and the ARRIVE guidelines.

2.18 | Statistical analysis

Data were analyzed using Graph Pad Prism 6.0 software. Statistical comparisons were evaluated using Student's *t* test and two-sway multiple-range analysis of variance. A *P*-value <.05 was considered statistically significant. All results are presented as means ± standard deviation.

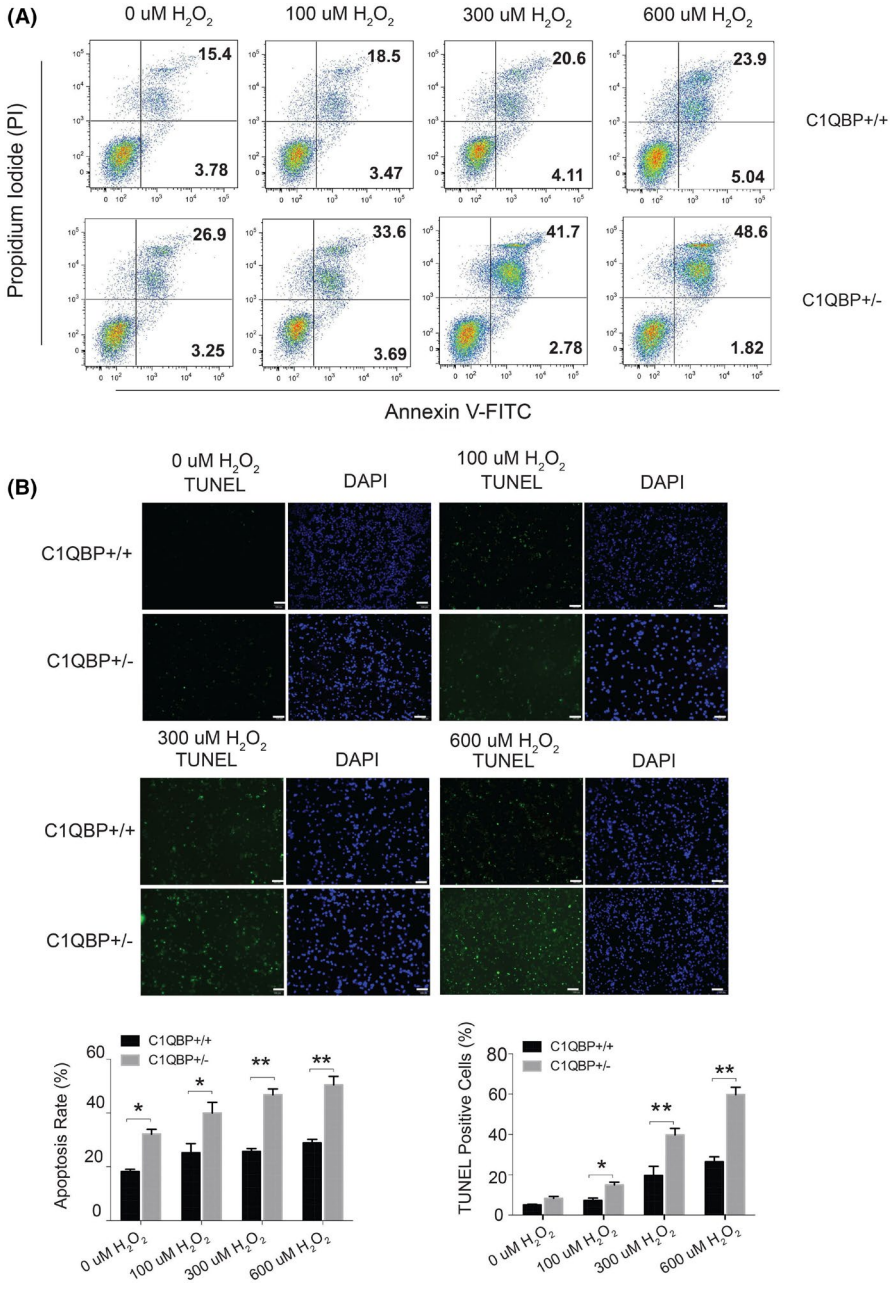

FIGURE 2 Complement C1q binding protein (C1QBP) knockdown aggravates T cells apoptosis. T cells isolated from C1QBP$^{+/-}$ and C1QBP$^{+/+}$ mice were stimulated with anti–CD3/CD28-induced T cell receptor (TCR) activation for 24 h and then treated with the different doses of H_2O_2 for 30 min. A, T cells apoptosis was measured by annexin V-FITC plus propidium iodide staining and FACS analysis. B, TUNEL assay was used to evaluate damaged DNA under the above experimental condition. Scale bar, 100 μm. Bars show the percentages of T cell apoptosis, including the early apoptotic (Annexin$^+$/PI$^-$) cells and the late apoptotic/dead (Annexin$^+$/PI$^+$) cells as well as TUNEL positive T cells in response to the H_2O_2 stimulation. Data are means ± standard deviation from three independent experiments (n = 3); $^{**}P < .01$, $^{*}P < .05$

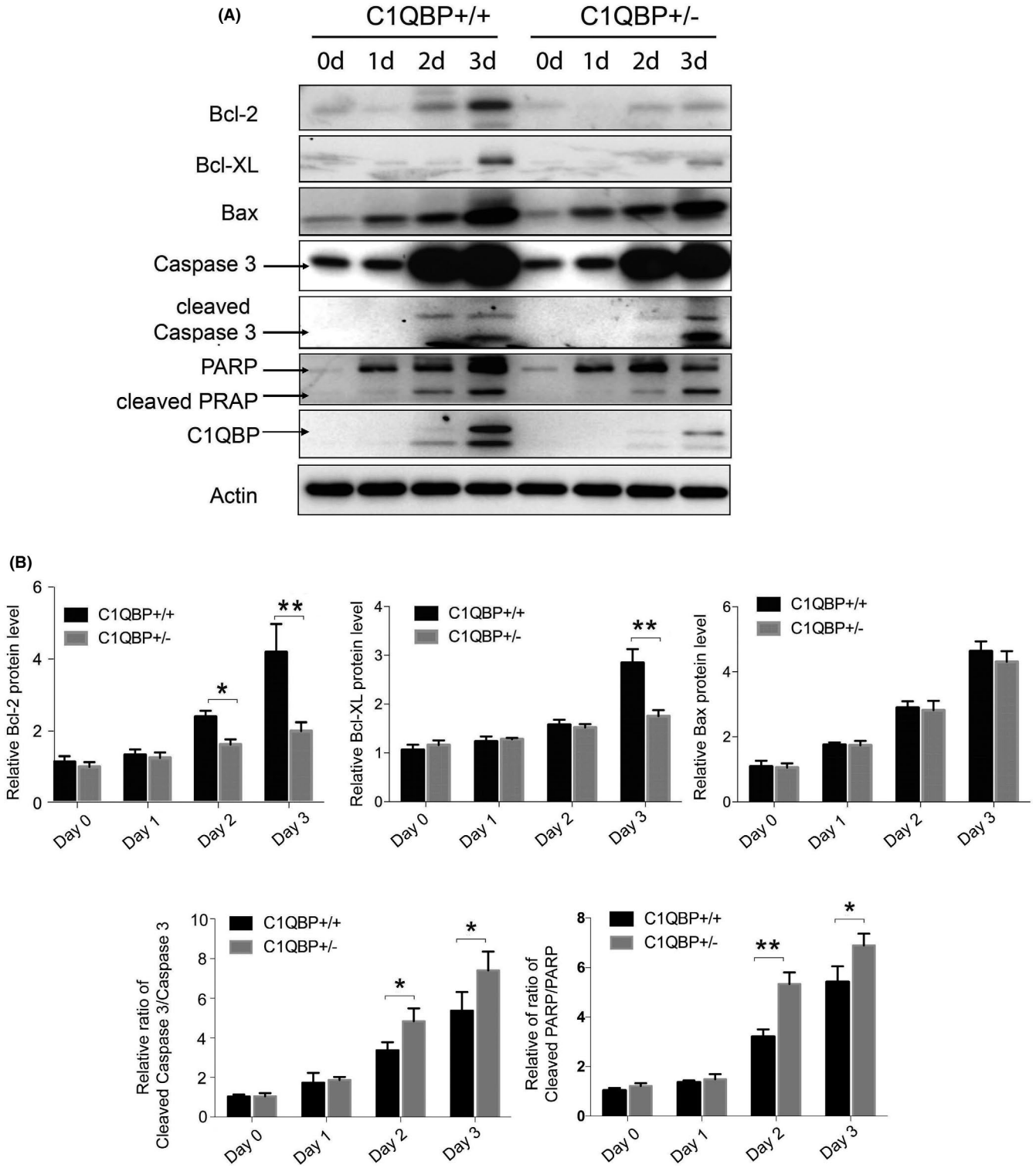

FIGURE 3 Complement C1q binding protein (C1QBP) knockdown impairs T cell apoptosis resistance through regulation of Bcl-2 family proteins. T cells isolated from C1QBP$^{+/+}$ and C1QBP$^{+/-}$ mice were stimulated with anti–CD3/CD28 antibodies for the indicated times. A, Protein levels of anti–apoptotic proteins, including Bcl-2 and Bcl-XL, pro–apoptotic executioner protein Bax, cleaved caspase-3, caspase-3, cleaved PARP, and PARP from C1QBP$^{+/+}$ and C1QBP$^{+/-}$ T cells, were analyzed by immunoblotting. B, Bars show the alteration of these above protein expressions. Data are means ± SD from three independent experiments (n = 3); $^{**}P < .01$, $^{*}P < .05$

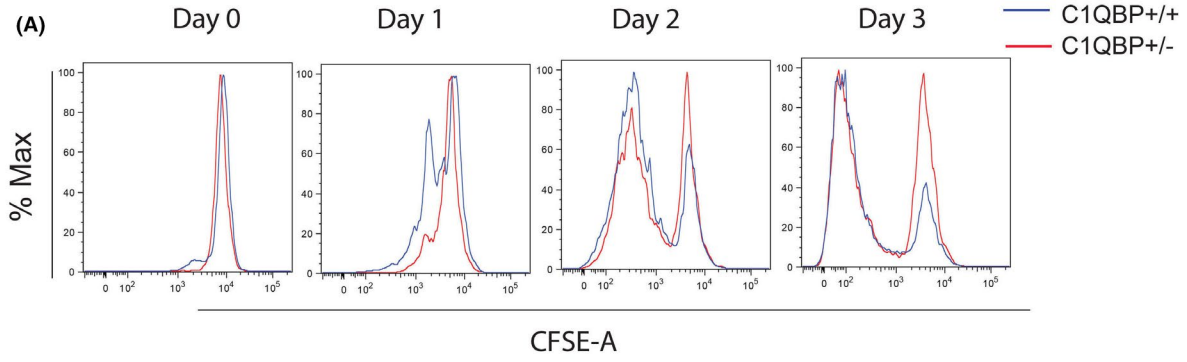
(A)
Day 0
Day 1
Day 2
Day 3
C1QBP+/+
C1QBP+/-
% Max
CFSE-A

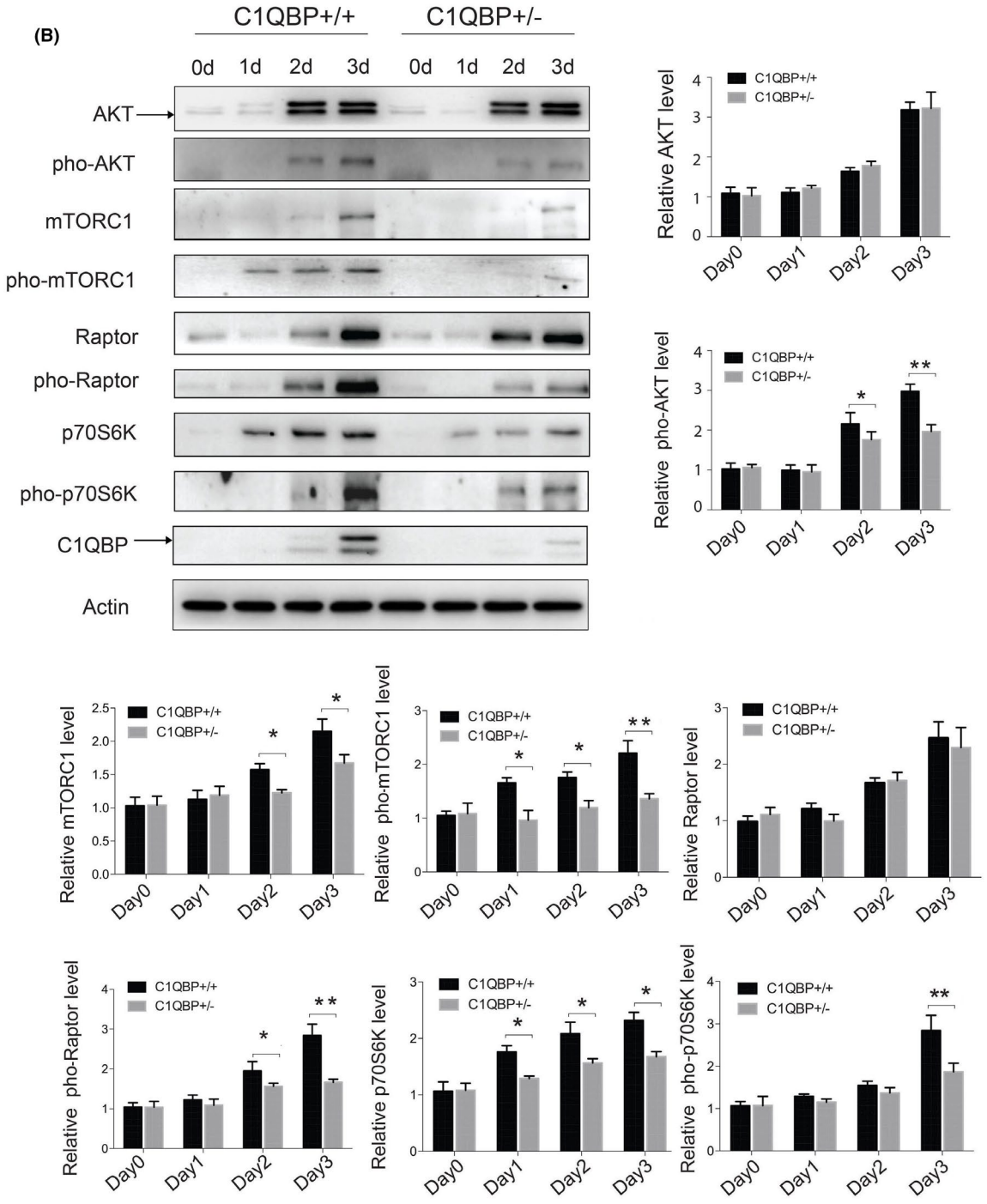
(B)
C1QBP+/+
C1QBP+/-
0d 1d 2d 3d 0d 1d 2d 3d
AKT
pho-AKT
mTORC1
pho-mTORC1
Raptor
pho-Raptor
p70S6K
pho-p70S6K
C1QBP
Actin
Relative AKT level
Relative pho-AKT level
Relative mTORC1 level
Relative pho-mTORC1 level
Relative Raptor level
Relative pho-Raptor level
Relative p70S6K level
Relative pho-p70S6K level
Day0
Day1
Day2
Day3

FIGURE 4 Complement C1q binding protein (C1QBP) knockdown suppresses T cell proliferation through regulation of the AKT-mTORC1 signaling pathway. T cells isolated from $C1QBP^{+/+}$ and $C1QBP^{+/-}$ mice were activated by anti–CD3/CD28 antibodies for the indicated times. A, T cell proliferation was assessed by carboxyfluorescein succinimidyl ester (CFSE) dilution assay using flow cytometry. Results are representative of three experiments. B, Protein levels of AKT, phospho-AKT (Ser473), mTORC1, phospho-mTORC1(Ser2448), Raptor, phospho-Raptor (Ser792), p70S6K, and phospho-p70S6K (Ser371) from $C1QBP^{+/+}$ and $C1QBP^{+/-}$ T cells were monitored by immunoblotting. The bar graphs show the means ± standard deviation of three independent experiments (n = 3); $^{**}P < .01$, $^{*}P < .05$

3 | RESULTS

3.1 | Complement C1q binding protein knockdown aggravates T cell apoptosis

Complement C1q binding protein plays an unignorable role in the maintenance of mitochondrial function and integrity.[12,14,15] At the same time, mitochondrial fitness is closely associated with T cell apoptosis upon extracellular adverse stresses.[4,9,10] Therefore, we wondered whether C1QBP would retain mitochondrial fitness to affect T cell apoptosis in response to TCR activation and ROS stress. As shown in Figure 1A, we isolated T cells from $C1QBP^{+/-}$ and $C1QBP^{+/+}$ mice to assess their ROS production after activation of the anti–CD3/CD28 antibody. We found that $C1QBP^{+/-}$ T cells exhibited more ROS production along with the extension of TCR activation. H_2O_2-induced oxidative stress also triggered more ROS accumulation in $C1QBP^{+/-}$ T cells when compared with the corresponding $C1QBP^{+/+}$ T cells. At the same time, the significant marker of mitochondrial dysfunction is the loss of mitochondrial membrane potential ($\Delta\Psi_M$). Here, the mitochondrial membrane potential was detected through TMRM assay and JC-10 assay, as shown in Figure 1B,C. $C1QBP^{+/-}$ T cells displayed more obvious loss of $\Delta\Psi_M$ than corresponding $C1QBP^{+/+}$ T cells under either TCR activation or H_2O_2 stimulation. These data suggested that C1QBP knockdown facilitated the decrease of $\Delta\Psi_M$ and exacerbated mitochondrial depolarization. In this regard, C1QBP is involved with the maintenance of mitochondrial fitness through reduction of ROS accumulation and prevention of $\Delta\Psi_M$ diminishment especially under the stimulation of TCR activation and oxidative stress.

Next, we continued to evaluate the apoptotic rate, including early apoptosis ($Annexin^+/PI^-$) and late apoptosis/death ($Annexin^+/PI^+$), under treatment of the different doses of H_2O_2. Our data showed that both $C1QBP^{+/+}$ and $C1QBP^{+/-}$ T cells had gradually increased apoptotic ratea accompanied by enhancement of H_2O_2 concentration. $C1QBP^{+/-}$ T cells displayed a more striking apoptotic phenotype from 30.15% (0 μM H_2O_2) to 50.42% (600 μM H_2O_2), whereas $C1QBP^{+/+}$ T cells exhibited relatively milder apoptosis from 19.18% (0 μM H_2O_2) to 28.94% (600 μM H_2O_2), as shown in Figure 2. Consequently, these data indicated that C1QBP knockdown partially deprived T cells of apoptosis resistance in response to ROS stress. Consistently, TUNEL assay also demonstrated that $C1QBP^{+/-}$ T cells possessed more damaged DNA than corresponding $C1QBP^{+/+}$ T cells, especially under treatment of 300 and 600 μM H_2O_2, which suggested that C1QBP knockdown rendered T cells prone to cellular apoptosis (Figure 2B).

Together, our data illustrated that $C1QBP^{+/-}$ T cells exhibited a ROS increase and $\Delta\Psi_M$ decrease when compared with $C1QBP^{+/+}$ T cells, suggesting that C1QBP knockdown impaired T cell mitochondrial fitness, making them susceptible to apoptosis.

3.2 | Complement C1q binding protein knockdown sensitizes T cells to apoptosis through regulation of Bcl-2 family proteins

Next, we explored the underlying mechanism of C1QBP knockdown on the regulation of T cell apoptosis. Anti–apoptotic members such as Bcl-2 were reported to impede the cellular apoptotic process through inhibiting the pro–apoptotic BH3-only proteins or binding the pro–apoptotic executioner proteins to prevent their oligomerization, thereby blocking mitochondrial outer membrane permeabilization (MOMP) and cytochrome c release into the cytosol.[24,25] Considering that Bcl-2 family proteins play a pivotal role in mitochondria-mediated apoptosis,[26-28] we thus asked whether C1QBP knockdown would sensitize T cells to apoptosis through regulation of Bcl-2 family proteins. As shown in Figure 3, our study demonstrated that less protein expression of the anti–apoptotic Bcl-2 family proteins, such as Bcl-2 and Bcl-XL, was detected in $C1QBP^{+/-}$ T cells in response to anti–CD3/CD28-induced TCR activation, although the pro–apoptotic executioner Bax exhibited a similar protein level.

Next, to further confirm that C1QBP is implicated in the mitochondria-mediated apoptosis of T cells, we assessed the downstream target proteins of the Bcl-2 signaling pathway, such as caspase-3 and PARP. The activation of caspase-3 contributed to the overall apoptotic morphology through cleavage of various cellular substrates.[29,30] In this study, we determined that TCR activation gradually enhanced the protein level of caspase-3 in both $C1QBP^{+/-}$ and $C1QBP^{+/+}$ T cells, as shown in Figure 3. However, $C1QBP^{+/-}$ T cells possessed more cleaved p17, an active subunit of caspase-3, and, thus, exhibited a higher relative ratio of cleaved caspase-3 versus caspase-3 when compared to $C1QBP^{+/+}$ T cells. Caspase-3 causes PARP cleavage and inactivation, which is also considered to be a hallmark of apoptosis.[31,32] Here, we found that $C1QBP^{+/-}$ T cells also showed a significantly higher ratio of cleaved PARP versus PARP, especially in response to stimulation of anti–CD3/CD28 antibodies for 3 days. Consequently, C1QBP knockdown aggravated caspase-3 cleavage to facilitate its downstream substrate PARP inactivation.

Together, the above data indicated that C1QBP knockdown decreased the protein expression of Bcl-2 and Bcl-XL, which further accelerated the involvement of the cleavage of caspase-3 and PARP with T cell apoptosis.

3.3 | Complement C1q binding protein knockdown suppresses T cell proliferation through dampening the AKT-mTORC1 signaling pathway

Upon activation, T cells adapt their metabolic reprogramming to meet the increased bioenergetic and biosynthetic demands during rapid proliferation and clonal expansion.[3,33,34] Furthermore, some studies have recently reported that mitochondrial function and fitness are indispensable for T cells to escape from quiescence as well as clonal expansion.[1,35] To explore whether C1QBP knockdown would impact T cell proliferation and uncover its underlying molecular mechanism, we detected the proliferation of C1QBP$^{+/-}$ and C1QBP$^{+/+}$ T cells and found that C1QBP knockdown obviously suppressed T cell proliferation along with activation of anti–CD3/CD28 antibodies (Figure 4A).

Given that mTOR, as the key metabolic regulator, integrates the extrinsic and intrinsic signals associated with nutrient levels, energy status, and stress to remodel mitochondrial metabolism for clonal expansion,[36-39] we further investigated whether C1QBP knockdown-mediated T cell proliferation decrease is at least partially attributed to the alteration of the AKT-mTORC1 signaling pathway. As shown in Figure 4B, although AKT protein expression demonstrated a gradual increase in both C1QBP$^{+/-}$ and C1QBP$^{+/+}$ T cells with the TCR activation, phosphorylation of AKT at Ser473 exhibited a smaller increase in C1QBP$^{+/-}$ T cells than the corresponding C1QBP$^{+/+}$ T cells. C1QBP$^{+/-}$ T cells also displayed weaker protein expression and phosphorylation of mTOR, Raptor and p70S6K. Together, these data suggested that C1QBP knockdown attenuated T cell proliferation, which is at least partially due to repression of the activation of the AKT-mTORC1 signaling pathway.

3.4 | Complement C1q binding protein knockdown impedes T cell tumor infiltration and exacerbates T cell exhaustion

Next, we utilized C1QBP$^{+/-}$ and C1QBP$^{+/+}$ mice injected with murine MC38 cells to investigate whether C1QBP knockdown would affect tumor progression. As shown in Figure 5A-C, we found that C1QBP$^{+/-}$ mice exhibited relatively stronger tumor progression when compared to the corresponding C1QBP$^{+/+}$ mice. We also assessed the expression of proliferation marker Ki67 and pro–apoptotic marker Puma in tumor tissues from C1QBP$^{+/-}$ and C1QBP$^{+/+}$ mice (Figure 5D). Our results showed that more Ki67 accumulated in the tumor tissues from C1QBP$^{+/-}$ mice, while more Puma was observed in the tumor tissues from C1QBP$^{+/+}$ mice, suggesting that the whole-body C1QBP knockdown exhibited more obvious tumor progression.

To further investigate whether T cells are at least partially responsible for the tumor progression of C1QBP$^{+/-}$ mice, we detected T cell tumor infiltration as well as exhaustion phenotype. Our data showed that the percentage of tumor-infiltrating C1QBP$^{+/-}$ T cells was approximately 1.47% (CD4$^+$) and 4.27% (CD8$^+$), while that of C1QBP$^{+/+}$ T cells was approximately 3.3% (CD4$^+$) and 7.8% (CD8$^+$), as shown in Figure 5E. Consistently, the immunohistochemistry staining also confirmed that fewer CD4$^+$ and CD8$^+$-positive C1QBP$^{+/-}$ T cells infiltrated the tumor microenvironment (TME) than the corresponding C1QBP$^{+/+}$ T cells (Figure 5F). Notably, some previous studies reported that impaired mitochondrial oxidative phosphorylation was sufficient to upregulate genes linked to T cell exhaustion.[8,9,40] Next, we further evaluate whether C1QBP knockdown-induced mitochondrial dysfunction would impact the exhausted phenotype of these tumor-infiltrating T cells (TIL). We assessed the exhaustion markers, such as PD-1, Tim-3, and LAG-3, in these tumor specific CD4$^+$ and CD8$^+$ T cells and found that these inhibitory receptors exhibited higher expression in tumor-infiltrating CD4$^+$ and CD8$^+$ C1QBP$^{+/-}$ T cells than the corresponding C1QBP$^{+/+}$ T cells, as shown in Figure 5G. In this regard, C1QBP knockdown actually retarded T cell tumor infiltration and exacerbated the TIL exhaustion, leading to a weaker anti–tumor immune response.

3.5 | Complement C1q binding protein knockdown impairs chimeric antigen receptor T cell anti–tumor immunotherapeutic efficacy

To further evaluate whether C1QBP may directly impact T cell-mediated immunotherapy, we designed CAR-modified T cells with different amounts of C1QBP. The B7-H3 protein has limited expression in normal human tissues, including liver, breast, and colon, whereas it is abnormally expressed in a high proportion of human malignancies.[41-44] Moreover, B7-H3, as one member of B7 immune co–stimulatory and co–inhibitory family, possesses two isoforms in humans, 2Ig-B7-H3 and 4Ig-B7-H3.[45,46] Here, we constructed the C1QBP$^{+/-}$ and C1QBP$^{+/+}$ CAR T cells targeting human B7-H3 (huB7-H3). Of course, we also transfected the MC38 cells with the lentivirus system expressing hu4Ig-B7-H3 to assess the anti–tumor immune function of C1QBP$^{+/-}$ and C1QBP$^{+/+}$ CAR T cells. The huB7-H3 MC38 cells were co–cultured with C1QBP$^{+/-}$ and

FIGURE 5 Complement C1q binding protein (C1QBP) knockdown impacts tumor progression. 2×10^5 MC38 cells were injected subcutaneously into the flanks of C1QBP$^{+/+}$ and C1QBP$^{+/-}$ mice (five mice per group). A, Representative bioluminescence images of MC38 xenograft tumors in C1QBP$^{+/+}$ and C1QBP$^{+/-}$ mice after 21 d of injection. B, Tumor tissues were collected from C1QBP$^{+/+}$ and C1QBP$^{+/-}$ mice after 21 d of injection. C, The bar graphs show the alterations of tumor volume and weight from C1QBP$^{+/+}$ and C1QBP$^{+/-}$ mice after 21 d of tumor injection. D, Ki67 (proliferation marker) and Puma (anti–apoptotic marker) expressed in tumor tissues from C1QBP$^{+/+}$ and C1QBP$^{+/-}$ mice were assessed by immunohistochemistry. Scale bars, 10 μm (200×), 5 μm (400×). E, The relative percentages of tumor-infiltrating CD4$^+$ and CD8$^+$ T cells from C1QBP$^{+/+}$ and C1QBP$^{+/-}$ mice were assessed by flow cytometry. F, The anti–CD4 and anti–CD8 antibodies were used to detect T cell tumor infiltration in C1QBP$^{+/+}$ and C1QBP$^{+/-}$ mice by immunohistochemistry. Scale bars, 10 μm (200×), 5 μm (400×). G, Exhaustion markers (PD1, Tim-3, LAG3) expressed in CD4$^+$ and CD8$^+$ T cells from C1QBP$^{+/+}$ and C1QBP$^{+/-}$ mice were assessed by flow cytometry. The bar graphs show the means ± SD of three independent experiments (n = 3); ***$P < .001$, **$P < .01$, *$P < .05$

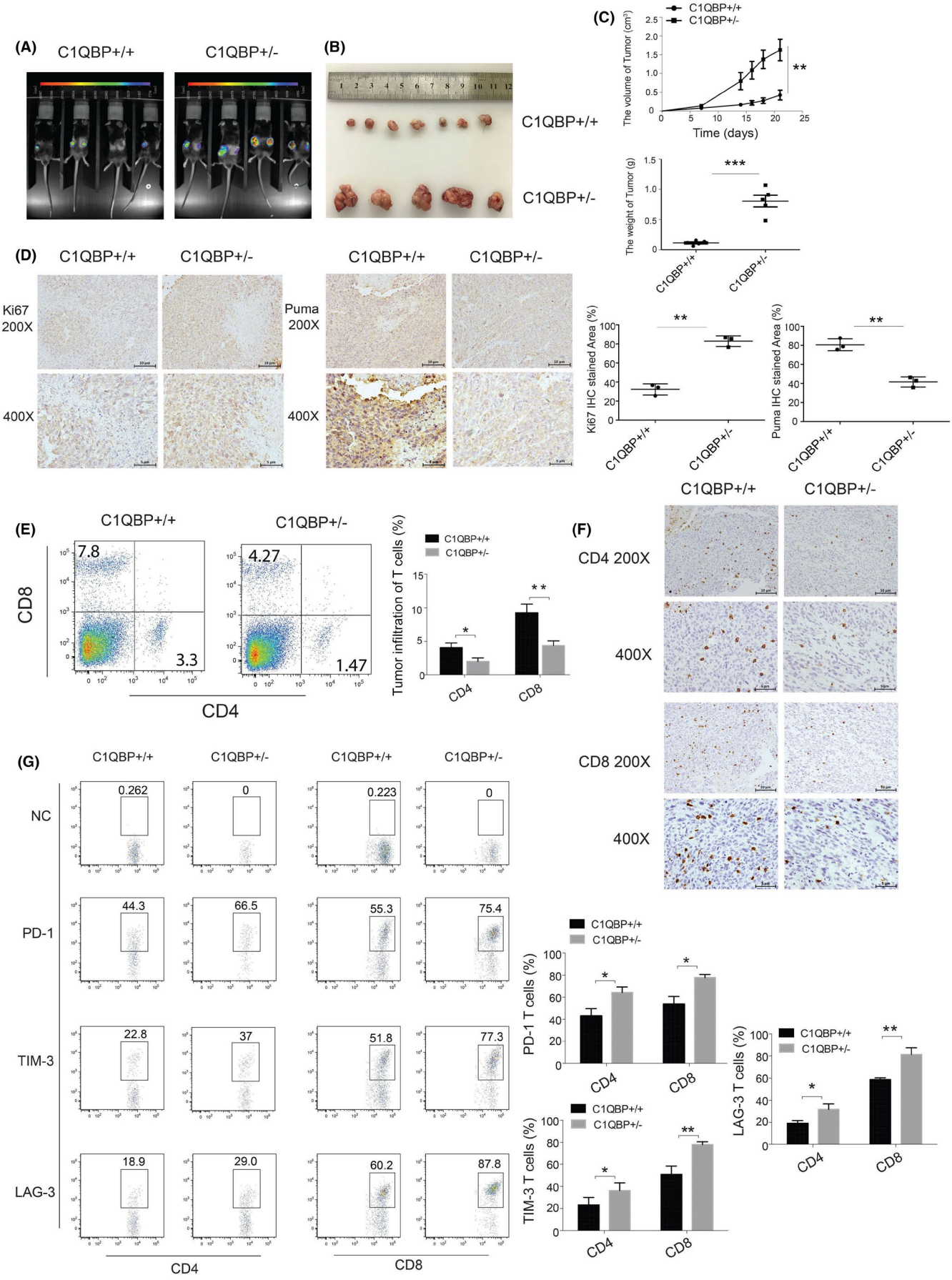
(A)
C1QBP+/+
C1QBP+/-
(B)
C1QBP+/+
C1QBP+/-
(C)
C1QBP+/+
C1QBP+/-
The volume of Tumor (cm3)
Time (days)
**
The weight of Tumor (g)
***
C1QBP+/+
C1QBP+/-
(D)
C1QBP+/+
C1QBP+/-
C1QBP+/+
C1QBP+/-
Ki67 200X
400X
Puma 200X
400X
Ki67 IHC stained Area (%)
Puma IHC stained Area (%)
**
**
C1QBP+/+
C1QBP+/-
C1QBP+/+
C1QBP+/-
(E)
C1QBP+/+
C1QBP+/-
CD8
CD4
7.8
3.3
4.27
1.47
Tumor infiltration of T cells (%)
C1QBP+/+
C1QBP+/-
*
**
CD4
CD8
(F)
C1QBP+/+
C1QBP+/-
CD4 200X
400X
CD8 200X
400X
(G)
C1QBP+/+
C1QBP+/-
C1QBP+/+
C1QBP+/-
NC
PD-1
TIM-3
LAG-3
0.262
0
0.223
0
44.3
66.5
55.3
75.4
22.8
37
51.8
77.3
18.9
29.0
60.2
87.8
CD4
CD8
PD-1 T cells (%)
TIM-3 T cells (%)
LAG-3 T cells (%)
C1QBP+/+
C1QBP+/-
*
*
**
**
**
CD4
CD8

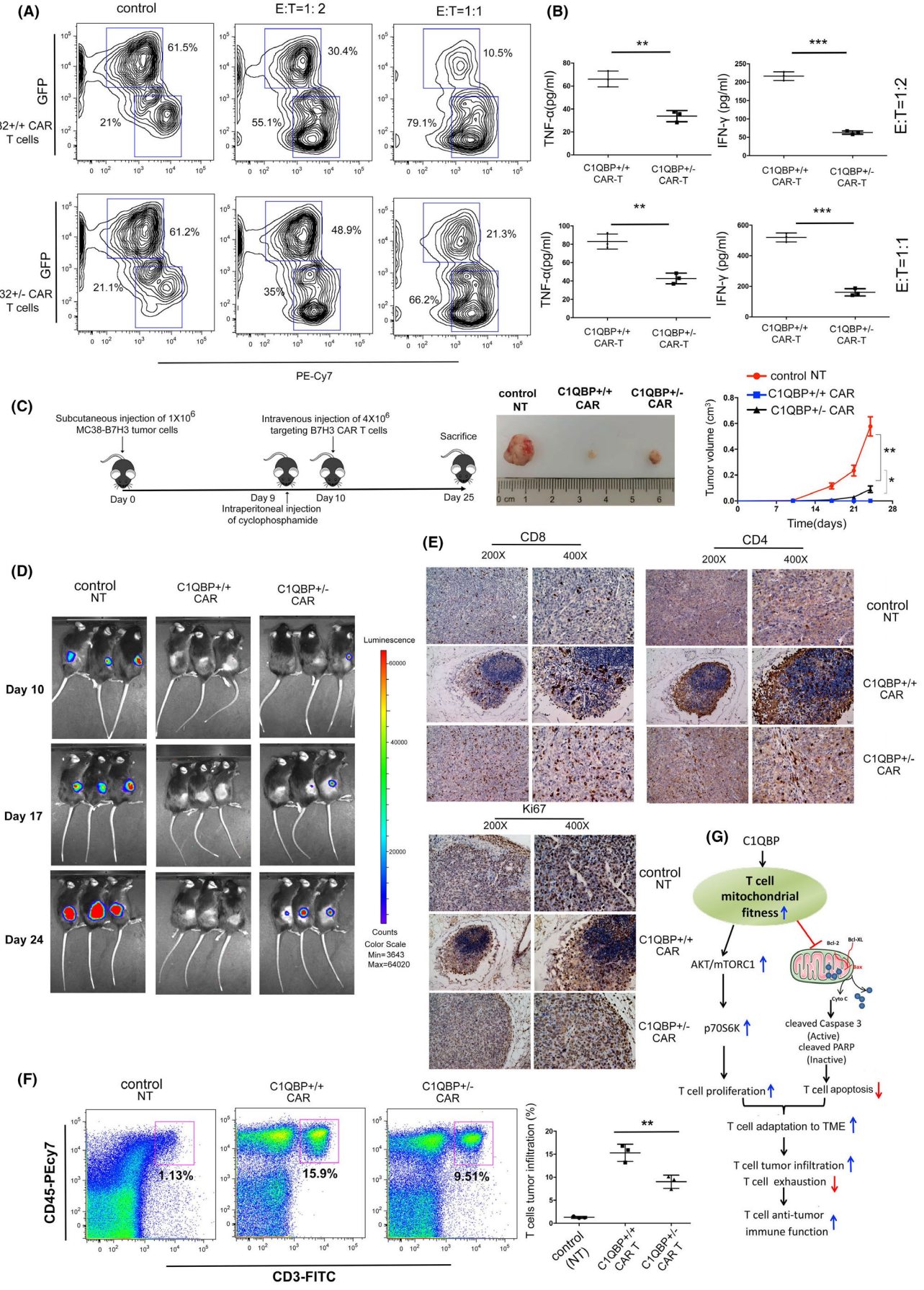
(A)
control
E:T=1: 2
E:T=1:1
GFP
p32+/+ CAR T cells
p32+/- CAR T cells
61.5%
21%
30.4%
55.1%
10.5%
79.1%
61.2%
21.1%
48.9%
35%
21.3%
66.2%
PE-Cy7
(B)
TNF-α(pg/ml)
IFN-γ (pg/ml)
C1QBP+/+ CAR-T
C1QBP+/- CAR-T
E:T=1:2
E:T=1:1
(C)
Subcutaneous injection of 1X10^6 MC38-B7H3 tumor cells
Intravenous injection of 4X10^6 targeting B7H3 CAR T cells
Sacrifice
Day 0
Day 9
Day 10
Day 25
Intraperitoneal injection of cyclophosphamide
control NT
C1QBP+/+ CAR
C1QBP+/- CAR
Tumor volume (cm3)
Time(days)
(D)
Day 10
Day 17
Day 24
Luminescence
Counts
Color Scale
Min=3643
Max=64020
(E)
CD8
CD4
Ki67
200X
400X
(F)
CD45-PEcy7
CD3-FITC
1.13%
15.9%
9.51%
T cells tumor infiltration (%)
control (NT)
(G)
C1QBP
T cell mitochondrial fitness
AKT/mTORC1
p70S6K
Bcl-2
Bcl-XL
Bax
Cyto C
cleaved Caspase 3 (Active)
cleaved PARP (Inactive)
T cell proliferation
T cell apoptosis
T cell adaptation to TME
T cell tumor infiltration
T cell exhaustion
T cell anti-tumor immune function

FIGURE 6 Complement C1q binding protein (C1QBP) knockdown impairs the anti–tumor immune function of chimeric antigen receptor (CAR) T cells in vivo and in vitro. A, The huB7-H3 MC38 cells (marked by green fluorescent protein [GFP]) were co–cultured with the control non–transduced T (NT) cells or the C1QBP$^{+/+}$ and C1QBP$^{+/-}$ CAR T cells (marked by PE-Cy7-CD3) at the different effector to target ratio (E:T = 1:2 or 1:1) for 6 h and were then evaluated by flow cytometry. B, IFN-γ and TNF-α in the co–culture supernatant (E:T = 1:2 or 1:1) were measured by ELISA. C, Schematic representation of the procedure in huB7-H3 MC38 subcutaneous xenograft mouse model adoptively transferred with CAR T cells. The representative picture and the calculation of tumor volumes from the C57BL/6 mice adoptively transferred with control NT, C1QBP$^{+/+}$ as well as C1QBP$^{+/-}$ CAR T cells on Day 24. D, Representative bioluminescence images of tumor progression in the huB7-H3 MC38 xenograft mouse model adoptively transferred with control NT, C1QBP$^{+/+}$, and C1QBP$^{+/-}$ CAR T cells on Days 10, 17, and 24 (three mice/group). E, The anti–CD4, CD8 and Ki67 antibodies were used for immunohistochemistry staining to detect T cell infiltration and tumor proliferation of the above three groups. Scale bars, 50 μm (200×), 20 μm (400×). F, The relative percentages of tumor-infiltrating T cells were assessed by flow cytometry. The FACS plots are representative for three independent experiments. G, Schematic model of C1QBP regulation of T cell mitochondrial fitness to potentiate their anti–tumor immune function. The static graphs show the means ± standard deviations of three independent experiments (n = 3); $^{***}P < .001$, $^{**}P < .01$, $^{*}P < .05$

C1QBP$^{+/+}$ CAR T cells at different effector to target (E:T) ratios. Our data demonstrated that C1QBP$^{+/-}$ CAR T cells exhibited relatively weaker immune function and repressed huB7-H3 MC38 cells to 48.9% (E:T = 1:2) and 21.3% (E:T = 1:1), while C1QBP$^{+/+}$ CAR T cells significantly limited huB7-H3 MC38 cells to 30.4% (E:T = 1:2) and 10.5% (E:T = 1:1), as shown in Figure 6A. Moreover, to compare the cytolytic activity of these CAR T cells, we detected the relative cytokines, including IFN-γ and TNF-α released in the culture supernatant, as shown in Figure 6B. Our data showed that C1QBP$^{+/-}$ CAR T cells generated relatively less IFN-γ and TNF-α when compared with C1QBP$^{+/+}$ CAR T cells, suggesting that C1QBP knockdown actually impaired the anti–tumor immune capacity of CAR T cells in vitro.

At the same time, we also investigated the exact role of C1QBP in the anti–tumor immune function of CAR T cells in vivo. We injected huB7-H3 MC38 cells into mice and then adoptively transferred the corresponding C1QBP$^{+/+}$ and C1QBP$^{+/-}$ CAR T cells to these mice. First, both C1QBP$^{+/+}$ and C1QBP$^{+/-}$ CAR T cell groups exhibited striking tumor suppression when compared to the control non–transduced T cell group. Second, we measured the volume of tumors and found that the CAR T cells with insufficient C1QBP had relatively weaker tumor regression than the CAR T cells with sufficient C1QBP, as shown in Figure 6C,D. At the same time, the immunohistochemistry results also confirmed that the C1QBP$^{+/-}$ CAR T cell group had fewer CD4^{+} and CD8^{+}-positive T cells infiltrating tumor tissues (Figure 6E). The data from flow cytometry also confirmed this conclusion, as shown in Figure 6F. Furthermore, greater expression of proliferation marker Ki67 was detected in the tumor tissues from C1QBP$^{+/-}$ CAR T cells group. Together, these data suggested that C1QBP knockdown actually attenuated the corresponding immunotherapeutic efficacy of CAR T cells.

4 | DISCUSSION

During the anti–tumor immune response, T cells transfer from nutrient-sufficient lymphoid organs to nutrient-deficient TME. Adaptation to the nutrient-restrictive environment is necessary for T cells to survive, proliferate, and perform their anti–tumor immune functions.[4,6] Metabolic insufficiency is a fundamental limitation by which environmental context dampens the TIL effector function to induce their tolerance as well as anergy.[5,6,47,48] Therefore, improvement of TIL mitochondrial fitness could be crucial to maintain their survival, proliferation, and effector function.

Indeed, previous studies using both gain- and loss-of-function approaches have demonstrated that C1QBP is implicated in the potentiation of mitochondrial metabolism.[14,17] In fact, C1QBP knockdown shifts cellular metabolism from oxidative phosphorylation toward aerobic glycolysis. In addition, C1QBP has been reported to be involved in the protection of mitochondrial dynamics and integrity.[16,49] For example, C1QBP knockdown induced mitochondrial fragmentation and fission in response to DNA damages treatment.[12,16,49,50] In this regard, C1QBP is indispensable for maintaining mitochondrial function and integrity. Here, our data also showed that one allele of C1QBP knocking out decreased T cells' mitochondrial membrane potential and increased their ROS accumulation, suggesting that C1QBP deficiency induced the impairment of T cell mitochondrial fitness. Besides, we found that C1QBP insufficiency attenuated T cell apoptotic resistance in response to TCR activation as well as ROS stress. To further explore the underlying mechanism, we evaluated the alteration of anti–apoptotic proteins, such as Bcl-2 and Bcl-XL, as well as pro–apoptotic executioner protein Bax. Although Bax has no obvious alteration in these T cells, C1QBP$^{+/-}$ T cells exhibited less accumulation of Bcl-2 and Bcl-XL when compared to C1QBP$^{+/+}$ T cells. Several studies have reported that Bax was constitutively active and oligomerized to induce MOMP, unless it was held in check by anti–apoptotic proteins like Bcl-2 and Bcl-XL.[27,28,51] Consequently, we presume that the decrease of Bcl-2 and Bcl-XL due to C1QBP knockdown probably fails to effectively sequestrate Bax and conversely facilitates MOMP process. Moreover, C1QBP knockdown also induced caspase-3 activation to initiate its downstream target PARP cleavage, which subsequently triggered the execution phase of T cell apoptosis. In this regard, C1QBP enhances the anti–apoptotic proteins like Bcl-2 and Bcl-XL to limit caspase-3 activation and PARP cleavage, which therefore resists T cell apoptosis through maintaining their mitochondrial fitness.

In addition to regulation of T cells apoptosis, we found that C1QBP knockdown suppresses T cell proliferation through dampening the AKT-mTORC1 signaling pathway. Some previous studies

have pointed out that mTORC1 is closely linked to mitochondrial function.[37,52-54] For example, genetic activation of mTORC1 through depletion of TSC2 may elevate mitochondrial function through mitochondrial biogenesis and oxidative metabolism.[52,54] Moreover, mTORC1 increased mitochondrial mass, mitochondrial DNA levels, and mitochondrial proteins translation, which correlated with high ATP production and increased mitochondrial function.[37,53,55] Consequently, whether C1QBP could be involved in the regulation of T cell mitochondrial metabolism and whether C1QBP would impact mitochondrial biogenesis through the activation of the AKT-mTORC1 signaling pathway are still intriguing questions.

A restrictive microenvironment forces T cells to utilize metabolic reprogramming for adaptation to the adverse stresses and to exert their anti–tumor immune functions. Metabolic insufficiency may be a fundamental mechanism by which TME inhibits T cells' tumor infiltration and their effector function.[6-8,40,56] In this study, C1QBP knockdown impeded $CD4^+$ and $CD8^+$ T cells' tumor infiltration and aggravated their exhausted phenotype through increasing co–inhibitory molecules such as PD-1, Tim-3, and LAG-3. Therefore, it is highly possible that C1QBP insufficiency results in the impairment of TIL mitochondrial fitness, which subsequently deprives these TIL of metabolic competition and attenuates their tumor infiltration as well as persistent immune efficacy. In contrast, some studies have reported that the enhancement of mitochondrial function endows TIL with the robust and durable effector function.[6,57] Notably, PGC1α was reported to regulate mitochondrial biogenesis and mitochondrial plasticity.[6,58,59] For example, overexpression of PGC1α could effectively rescue exhausted T cells due to their metabolic insufficiency. PGC1α significantly potentiated effector function of these hyporesponsive T cells through augment of mitochondrial biogenesis.[59] The enhancement of PGC1α obviously reversed PD-1-induced bioenergetic insufficiencies and renovated T cells' immune function.[60] Consequently, whether the involvement of C1QBP in the regulation of mitochondrial biogenesis via PGC1α and C1QBP knockdown-mediated TIL exhaustion is partially attributed to the decrease of mitochondrial biogenesis warrants further investigation. Finally, we constructed huB7-H3 targeted CAR T cells with a different amount of C1QBP to further confirm the exact role of C1QBP on T cell-related immunotherapy. Our results demonstrated that the $C1QBP^{+/-}$ CAR T cells had relatively weaker tumor repression in vivo and in vitro than the corresponding $C1QBP^{+/+}$ CAR T cells. In other words, C1QBP knockdown rendered CAR T cells with lower anti–tumor immunotherapeutic efficacy through diminishment of their tumor infiltration and immune cytolytic activity. Potentiation of the mitochondrial fitness through C1QBP could be an attractive approach to acquire persistent adaptation to the relentless TME and enhance CAR T cells' anti–tumor immune function.[61,62]

Taken together, as shown in Figure 6G, C1QBP, as an important modulator to maintain mitochondrial fitness, is involved in regulation of T cell proliferation and anti–apoptosis. On the one hand, C1QBP promotes T cell rapid proliferation through activation of the AKT-mTORC1 signaling pathway. On the other hand, C1QBP improves T cells\ survival through recruitment of anti–apoptotic proteins, such as Bcl-2 and Bcl-XL, thus inhibiting caspase-3 cleavage and its downstream PARP inactivation. Finally, C1QBP endows T cells with enhanced mitochondrial adaptation to relentless TME through promotion of their tumor infiltration and repression of TIL exhaustion, thereby ensuring T cells exert a robust and persistent anti–tumor immune function. Although mitochondria underlie the fate and function of T cells, metabolic interventions for manipulating immunity are rare and can be considered to represent a largely untapped opportunity. Therefore, development of strategies for potentiation of T cells' mitochondrial fitness and metabolic plasticity through C1QBP could improve immunotherapeutic efficacy for tumor treatment.

ACKNOWLEDGMENTS

This study was supported by the National Natural Science Foundation of China (No. 82073012, 81871869, and 81872488) and the Key University Science Research Project of Jiangsu Province (No. 19KJA580001 and 19KJA470001).

DISCLOSURE

The authors declare that they have no conflicts of interest.

ORCID

Gang Wang https://orcid.org/0000-0001-6020-7263
Guan Jiang https://orcid.org/0000-0002-0705-2386
Junnian Zheng https://orcid.org/0000-0003-0208-6410

REFERENCES

1. Dimeloe S, Burgener AV, Grahlert J, Hess C. T-cell metabolism governing activation, proliferation and differentiation; a modular view. *Immunology*. 2017;150:35-44.
2. MacIver NJ, Michalek RD, Rathmell JC. Metabolic regulation of T lymphocytes. *Annu Rev Immunol*. 2013;31:259-283.
3. Pearce EL, Pearce EJ. Metabolic pathways in immune cell activation and quiescence. *Immunity*. 2013;38:633-643.
4. Chang C-H, Qiu J, O'Sullivan D, et al. Metabolic competition in the tumor microenvironment is a driver of cancer progression. *Cell*. 2015;162:1229-1241.
5. Crespo J, Sun H, Welling TH, Tian Z, Zou W. T cell anergy, exhaustion, senescence, and stemness in the tumor microenvironment. *Curr Opin Immunol*. 2013;25:214-221.
6. Scharping NE, Menk AV, Moreci RS, et al. The tumor microenvironment represses T cell mitochondrial biogenesis to drive intratumoral T cell metabolic insufficiency and dysfunction. *Immunity*. 2016;45:374-388.
7. Yu Y-R, Imrichova H, Wang H, et al. Disturbed mitochondrial dynamics in CD8(+) TILs reinforce T cell exhaustion. *Nat Immunol*. 2020;21:1540-1551.
8. Vardhana SA, Hwee MA, Berisa M, et al. Impaired mitochondrial oxidative phosphorylation limits the self-renewal of T cells exposed to persistent antigen. *Nat Immunol*. 2020;21:1022-1033.
9. Liu X, Peng G. Mitochondria orchestrate T cell fate and function. *Nat Immunol*. 2021;22:276-278.
10. Buck M, O'Sullivan D, Klein Geltink R, et al. Mitochondrial dynamics controls T cell fate through metabolic programming. *Cell*. 2016;166:63-76.

11. Jiang J, Zhang Y, Krainer AR, Xu RM. Crystal structure of human p32, a doughnut-shaped acidic mitochondrial matrix protein. *Proc Natl Acad Sci USA*. 1999;96:3572-3577.
12. Hu M, Crawford SA, Henstridge DC, et al. p32 protein levels are integral to mitochondrial and endoplasmic reticulum morphology, cell metabolism and survival. *Biochem J*. 2013;453:381-391.
13. Soltys BJ, Kang D, Gupta RS. Localization of P32 protein (gC1q-R) in mitochondria and at specific extramitochondrial locations in normal tissues. *Histochem Cell Biol*. 2000;114:245-255.
14. Fogal V, Richardson AD, Karmali PP, Scheffler IE, Smith JW, Ruoslahti E. Mitochondrial p32 protein is a critical regulator of tumor metabolism via maintenance of oxidative phosphorylation. *Mol Cell Biol*. 2010;30:1303-1318.
15. Yagi M, Uchiumi T, Takazaki S, et al. p32/gC1qR is indispensable for fetal development and mitochondrial translation: importance of its RNA-binding ability. *Nucleic Acids Res*. 2012;40:9717-9737.
16. Noh S, Phorl S, Naskar R, et al. p32/C1QBP regulates OMA1-dependent proteolytic processing of OPA1 to maintain mitochondrial connectivity related to mitochondrial dysfunction and apoptosis. *Sci Rep*. 2020;10:10618.
17. Gotoh K, Morisaki T, Setoyama D, et al. Mitochondrial p32/C1qbp is a critical regulator of dendritic cell metabolism and maturation. *Cell Rep*. 2018;25:1800-1815 e1804.
18. Ling GS, Crawford G, Buang N, et al. C1q restrains autoimmunity and viral infection by regulating CD8(+) T cell metabolism. *Science*. 2018;360:558-563.
19. Liu Y, Leslie PL, Jin A, Itahana K, Graves LM, Zhang Y. p32 heterozygosity protects against age- and diet-induced obesity by increasing energy expenditure. *Sci Rep*. 2017;7:5754.
20. Itahana K, Mao H, Jin A, et al. Targeted inactivation of Mdm2 RING finger E3 ubiquitin ligase activity in the mouse reveals mechanistic insights into p53 regulation. *Cancer Cell*. 2007;12:355-366.
21. Bai J, Yong H-M, Chen F-F, et al. RUNX3 is a prognostic marker and potential therapeutic target in human breast cancer. *J Cancer Res Clin Oncol*. 2013;139:1813-1823.
22. Kochenderfer JN, Yu Z, Frasheri D, Restifo NP, Rosenberg SA. Adoptive transfer of syngeneic T cells transduced with a chimeric antigen receptor that recognizes murine CD19 can eradicate lymphoma and normal B cells. *Blood*. 2010;116:3875-3886.
23. Du H, Hirabayashi K, Ahn S, et al. Antitumor responses in the absence of toxicity in solid tumors by targeting B7–H3 via chimeric antigen receptor T cells. *Cancer Cell*. 2019;35:221-237 e228.
24. Youle RJ, Strasser A. The BCL-2 protein family: opposing activities that mediate cell death. *Nat Rev Mol Cell Biol*. 2008;9:47-59.
25. Tait SW, Green DR. Mitochondria and cell death: outer membrane permeabilization and beyond. *Nat Rev Mol Cell Biol*. 2010;11:621-632.
26. Shamas-Din A, Kale J, Leber B, Andrews DW. Mechanisms of action of Bcl-2 family proteins. *Cold Spring Harb Perspect Biol*. 2013;5:a008714.
27. Vela L, Gonzalo O, Naval J, Marzo I. Direct interaction of Bax and Bak proteins with Bcl-2 homology domain 3 (BH3)-only proteins in living cells revealed by fluorescence complementation. *J Biol Chem*. 2013;288:4935-4946.
28. Ku B, Liang C, Jung JU, Oh BH. Evidence that inhibition of BAX activation by BCL-2 involves its tight and preferential interaction with the BH3 domain of BAX. *Cell Res*. 2011;21:627-641.
29. Porter AG, Janicke RU. Emerging roles of caspase-3 in apoptosis. *Cell Death Differ*. 1999;6:99-104.
30. McIlwain DR, Berger T, Mak TW. Caspase functions in cell death and disease. *Cold Spring Harb Perspect Biol*. 2013;5:a008656.
31. Los M, Mozoluk M, Ferrari D, et al. Activation and caspase-mediated inhibition of PARP: a molecular switch between fibroblast necrosis and apoptosis in death receptor signaling. *Mol Biol Cell*. 2002;13:978-988.
32. Soldani C, Scovassi AI. Poly(ADP-ribose) polymerase-1 cleavage during apoptosis: an update. *Apoptosis*. 2002;7:321-328.
33. Buck MD, O'Sullivan D, Pearce EL. T cell metabolism drives immunity. *J Exp Med*. 2015;212:1345-1360.
34. Desdin-Mico G, Soto-Heredero G, Mittelbrunn M. Mitochondrial activity in T cells. *Mitochondrion*. 2018;41:51-57.
35. Chapman NM, Boothby MR, Chi H. Metabolic coordination of T cell quiescence and activation. *Nat Rev Immunol*. 2020;20:55-70.
36. Laplante M, Sabatini DM. mTOR signaling in growth control and disease. *Cell*. 2012;149:274-293.
37. Khan NA, Nikkanen J, Yatsuga S, et al. mTORC1 regulates mitochondrial integrated stress response and mitochondrial myopathy progression. *Cell Metab*. 2017;26:419-428 e415.
38. Chi H. Regulation and function of mTOR signalling in T cell fate decisions. *Nat Rev Immunol*. 2012;12:325-338.
39. Mondino A, Mueller DL. mTOR at the crossroads of T cell proliferation and tolerance. *Semin Immunol*. 2007;19:162-172.
40. Scharping NE, Rivadeneira DB, Menk AV, et al. Mitochondrial stress induced by continuous stimulation under hypoxia rapidly drives T cell exhaustion. *Nat Immunol*. 2021;22:205-215.
41. Seaman S, Zhu Z, Saha S, et al. Eradication of tumors through simultaneous ablation of CD276/B7-H3-positive tumor cells and tumor vasculature. *Cancer Cell*. 2017;31:501-515 e508.
42. Inamura K, Yokouchi Y, Kobayashi M, et al. Tumor B7–H3 (CD276) expression and smoking history in relation to lung adenocarcinoma prognosis. *Lung Cancer*. 2017;103:44-51.
43. Hofmeyer KA, Ray A, Zang X. The contrasting role of B7–H3. *Proc Natl Acad Sci USA*. 2008;105:10277-10278.
44. Picarda E, Ohaegbulam KC, Zang X. Molecular pathways: targeting B7–H3 (CD276) for human cancer immunotherapy. *Clin Cancer Res*. 2016;22:3425-3431.
45. Steinberger P, Majdic O, Derdak SV, et al. Molecular characterization of human 4Ig-B7-H3, a member of the B7 family with four Ig-like domains. *J Immunol*. 2004;172:2352-2359.
46. Chapoval AI, Ni J, Lau JS, et al. B7–H3: a costimulatory molecule for T cell activation and IFN-gamma production. *Nat Immunol*. 2001;2:269-274.
47. Yi JS, Cox MA, Zajac AJ. T-cell exhaustion: characteristics, causes and conversion. *Immunology*. 2010;129:474-481.
48. Saeidi A, Zandi K, Cheok YY, et al. T-cell exhaustion in chronic infections: reversing the state of exhaustion and reinvigorating optimal protective immune responses. *Front Immunol*. 2018;9:2569.
49. Li Y, Wan OW, Xie W, Chung KK. p32 regulates mitochondrial morphology and dynamics through parkin. *Neuroscience*. 2011;199:346-358.
50. McGee AM, Baines CP. Complement 1q-binding protein inhibits the mitochondrial permeability transition pore and protects against oxidative stress-induced death. *Biochem J*. 2011;433:119-125.
51. Charo J, Finkelstein SE, Grewal N, Restifo NP, Robbins PF, Rosenberg SA. Bcl-2 overexpression enhances tumor-specific T-cell survival. *Cancer Res*. 2005;65:2001-2008.
52. Morita M, Gravel S-P, Chénard V, et al. mTORC1 controls mitochondrial activity and biogenesis through 4E-BP-dependent translational regulation. *Cell Metab*. 2013;18:698-711.
53. Cunningham JT, Rodgers JT, Arlow DH, Vazquez F, Mootha VK, Puigserver P. mTOR controls mitochondrial oxidative function through a YY1-PGC-1alpha transcriptional complex. *Nature*. 2007;450:736-740.
54. de la Cruz Lopez KG, Toledo Guzman ME, Sanchez EO, Garcia CA. mTORC1 as a regulator of mitochondrial functions and a therapeutic target in cancer. *Front Oncol*. 2019;9:1373.
55. Bentzinger CF, Romanino K, Cloëtta D, et al. Skeletal muscle-specific ablation of raptor, but not of rictor, causes metabolic changes and results in muscle dystrophy. *Cell Metab*. 2008;8:411-424.
56. Sugiura A, Rathmell JC. Metabolic barriers to T cell function in tumors. *J Immunol*. 2018;200:400-407.
57. Le Bourgeois T, Strauss L, Aksoylar H-I, et al. Targeting T cell metabolism for improvement of cancer immunotherapy. *Front Oncol*. 2018;8:237.

58. Fernandez-Marcos PJ, Auwerx J. Regulation of PGC-1alpha, a nodal regulator of mitochondrial biogenesis. *Am J Clin Nutr*. 2011;93:884S-90.
59. Dumauthioz N, Tschumi B, Wenes M, et al. Enforced PGC-1alpha expression promotes CD8 T cell fitness, memory formation and antitumor immunity. *Cell Mol Immunol*. 2021;18(7):1761-1771.
60. Bengsch B, Johnson AL, Kurachi M, et al. Bioenergetic insufficiencies due to metabolic alterations regulated by the inhibitory receptor PD-1 are an early driver of CD8(+) T cell exhaustion. *Immunity*. 2016;45:358-373.
61. Rad SMA, Halpin JC, Mollaei M, Smith Bell SWJ, Hirankarn N, McLellan AD. Metabolic and mitochondrial functioning in chimeric antigen receptor (CAR)-T cells. *Cancers (Basel)*. 2021;13:1229.
62. van Bruggen JAC, Martens AWJ, Fraietta JA, et al. Chronic lymphocytic leukemia cells impair mitochondrial fitness in CD8(+) T cells and impede CAR T-cell efficacy. *Blood*. 2019;134:44-58.

How to cite this article: Tian H, Wang G, Wang Q, et al. Complement C1q binding protein regulates T cells' mitochondrial fitness to affect their survival, proliferation, and anti–tumor immune function. *Cancer Sci*. 2022;113:875–890. doi:10.1111/cas.15261